

Cite this article as: Zhou Yanxia, Li Wei, Fu Xiaokun, et al. Effects of Y and Zr Doping on Microstructure and Magnetic Properties for CeFeB Alloy[J]. Rare Metal Materials and Engineering, 2021, 50(09): 3139-3143.

ARTICLE

Effects of Y and Zr Doping on Microstructure and Magnetic Properties for CeFeB Alloy

Zhou Yanxia, Li Wei, Fu Xiaokun, Hou Yuhua, Huang Youlin

School of Materials Science and Engineering, Nanchang Hangkong University, Nanchang 330063, China

Abstract: Effects of Y and Zr doping on the phase constituent, magnetic properties, and temperature stability for CeFeB alloy were investigated. The results show that CeYFeB alloy consists of the 2:14:1 main phase and a small amount of α -Fe phase. Magnetic properties including coercivity, remanence, and magnetic product energy improve considerably after Y doping. Meanwhile, the temperature stability is enhanced significantly. Due to the excellent intrinsic magnetic properties and higher temperature stability of $Y_2Fe_{14}B$ phase, the remanence and coercivity temperature coefficients are $-0.32\%/K$ and $-0.41\%/K$, increasing by 38.5% and 40.6%, respectively, compared to those of the pure CeFeB alloy. After the Y and Zr co-doping, the coercivity, remanence, and magnetic product energy improve greatly, increasing by 30.9%, 58.1%, and 204.8%, respectively, compared to those of pure CeFeB alloy, because of the joint effects of enhanced magnet crystalline anisotropic field and refined grain size.

Key words: CeFeB alloy; Y doping; Zr doping; magnetic properties

NdFeB-based permanent magnets have been widely applied to various fields due to their excellent magnetic properties at room temperature^[1,2]. Due to the high cost and gradual decrease of rare earth resources, such as Nd, Pr, and Dy, the large amount of rare earth consumption for NdFeB-based magnets causes great concern about the sustainable development^[3]. However, the abundant rare earth element Ce is not widely used for permanent magnets due to the inferior intrinsic magnetic properties of $Ce_2Fe_{14}B$ compound (saturation magnetic polarization $J_s=1.17$ T, anisotropy field $H_a=2.6$ T, Curie temperature $T_c=151$ °C), which are not attractive compared with the properties of $Nd_2Fe_{14}B$ compound ($J_s=1.60$ T, $H_a=7.30$ T, $T_c=312$ °C)^[4]. Recently, it is reported that the coercivity of Nd-Ce-Fe-B alloys fabricated via melt spinning technique increases when the Ce content is 20at%^[5,6], which is attributed to the phase segregation behavior. In addition, the variation of Ce valence has an important effect on the magnetic properties^[7]. In terms of conventional sintered magnets, the maximum magnetic energy product of 342.28 kJ·m⁻³ was obtained through dual-alloy method^[8] when 30at% Ce is substituted for Nd, indicating the application potential of Ce

in rare earth permanent magnets.

Although $Y_2Fe_{14}B$ compound possesses inferior intrinsic magnetic properties ($J_s=1.41$ T, $H_a=2.0$ T), its application in permanent magnets still shows great potential due to its stable performance at high temperature^[9]. Zhang et al^[10] found that Y substitution for Nd increases remanence and magnetic product energy of exchange-coupled (Nd, Y)₂Fe₁₄B/ α -Fe alloy prepared by high-energy ball milling. Few studies investigated the substitution of Y for Ce in CeFeB alloy. In addition, it is proved that the addition of high melting point elements in NdFeB alloy, such as Zr^[11], Nb^[12], and Ti^[13], improves the microstructure, thereby enhancing the magnetic properties. In this research, the effects of Y and Zr doping on the microstructure and magnetic properties of CeFeB alloy were investigated in detail.

1 Experiment

(Ce_{1-x}Y_x)_{13.5}Fe_{81-y}B_{5.5}Zr_y ($x=0\sim 0.225$, $y=0\sim 3.0$, at%) ribbons were prepared by arc melting followed by melt spinning under Ar atmosphere with a velocity of 40 m/s. Each ingot was remelted at least 4 times to ensure the component

Received date: September 22, 2020

Foundation item: National Natural Science Foundation of China (51961027, 51564037, 51401103); Key Research and Development Program of Jiangxi Province (20181ACE50005, 20192ACB50020)

Corresponding author: Huang Youlin, Ph. D., Professor, School of Materials Science and Engineering, Nanchang Hangkong University, Nanchang 330063, P. R. China, Tel: 0086-791-86453209, E-mail: hyl1019_lin@163.com

Copyright © 2021, Northwest Institute for Nonferrous Metal Research. Published by Science Press. All rights reserved.

homogeneity. X-ray diffraction (XRD) patterns were collected by an ADVANCE D8 diffractometer (BRUKER/AXS, Germany). Microstructure was characterized by scanning electronic microscopy (SEM, FEI Quanta FEG 250). Magnetic properties were tested using a physical properties measurement system (PPMS-DynaCool, Quantum Design, USA) equipped with a vibrating sample magnetometer (VSM) of 9 T.

2 Results and Discussion

2.1 Effects of Y doping on magnetic properties and thermal stability

Fig.1 shows the XRD patterns for $(\text{Ce}_{1-x}\text{Y}_x)_{13.5}\text{Fe}_{81}\text{B}_{5.5}$ ($x=0\sim 0.225$) melt-spun alloys. Most diffraction peaks can be indexed as the 2:14:1 phase for all Y-doped alloys, and a small amount of α -Fe phase can also be observed. Magnetic hysteresis loops of $(\text{Ce}_{1-x}\text{Y}_x)_{13.5}\text{Fe}_{81}\text{B}_{5.5}$ alloys are shown in Fig. 2. The coercivity, remanence, and magnetic product energy of pure CeFeB alloy are 311 kA/m, 0.43 T, and 21 kJ/m³, respectively. There is no “step” phenomenon in the second quadrant demagnetization curves when x equals 0.075 and 0.175, meaning that α -Fe phase is well exchanged to the 2:14:1 phase. Detailed magnetic properties and their variation with respect to Y content are demonstrated in Fig.2 and Table 1. With increasing the Y content, the remanence (J) increases to 0.76 T ($x=0.175$) and then decreases. Compared to the saturation magnetization M_s of $\text{Ce}_2\text{Fe}_{14}\text{B}$ (1.17 T), M_s of $\text{Y}_2\text{Fe}_{14}\text{B}$ phase (1.41 T) is higher and responsible to the remanence increment. However, the weakened exchange coupling effect may be the main reason of degraded remanence, which is verified by the “step” phenomenon in the second quadrant demagnetization curve.

Many factors including intrinsic magnet crystalline anisotropic field, microstructure, and phase constituent can all produce crucial influence on coercivity. In this work, the highest coercivity of 411 kA/m is achieved, increasing by 32.2% compared to that of pure CeFeB alloy. The variation of coercivity between 311~411 kA/m should be attributed to the joint effects from magnet crystalline anisotropic field, microstructure, and phase constituent. The highest magnetic

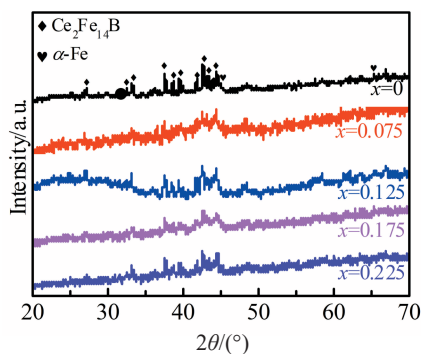


Fig.1 XRD patterns of $(\text{Ce}_{1-x}\text{Y}_x)_{13.5}\text{Fe}_{81}\text{B}_{5.5}$ ($x=0\sim 0.225$) melt-spun alloys

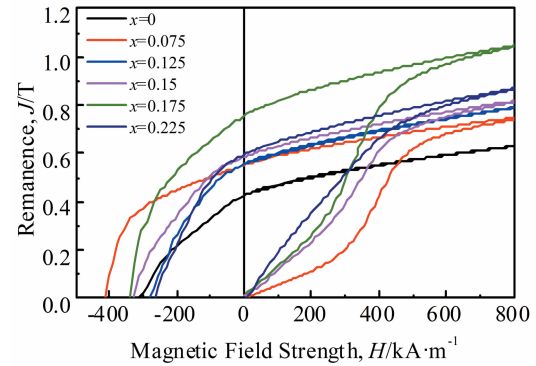


Fig.2 Magnetic hysteresis loops of $(\text{Ce}_{1-x}\text{Y}_x)_{13.5}\text{Fe}_{81}\text{B}_{5.5}$ alloys ($x=0\sim 0.225$)

Table 1 Magnetic properties of $(\text{Ce}_{1-x}\text{Y}_x)_{13.5}\text{Fe}_{81}\text{B}_{5.5}$ alloys ($x=0\sim 0.225$)

x	0	0.075	0.125	0.15	0.175	0.225
Coercivity, $H_{ci}/\text{kA}\cdot\text{m}^{-1}$	311	411	283	330	342	267
Remanence, J/T	0.43	0.55	0.54	0.59	0.76	0.60
Magnetic energy product, $BH_{\text{max}}/\text{kJ}\cdot\text{m}^{-3}$	21	43	32	39	61	36

product energy reaches 61 kJ/m³, increasing by 190.5% compared to that of pure CeFeB alloy. Overall, the optimal comprehensive magnetic properties with the coercivity of 342 kA/m, remanence of 0.76 T, and magnetic energy product of 61 kJ/m³ are achieved, increasing by 9.97%, 76.7%, and 190.5%, respectively. It is concluded that the appropriate addition of Y effectively improves the magnetic properties of Ce-Fe-B alloy.

Temperature stability is evaluated by the temperature coefficient of remanence and coercivity, which is determined by Eq.(1) and Eq.(2), respectively^[14,15]:

$$\alpha = [J(T) - J(T_0)] / J(T_0)(T - T_0) \times 100\% \quad (1)$$

$$\beta = [H_{ci}(T) - H_{ci}(T_0)] / H_{ci}(T_0)(T - T_0) \times 100\% \quad (2)$$

where α is temperature coefficient of remanence, β is temperature coefficient of coercivity, T is the temperature stability, and T_0 is initial temperature.

The dependence of remanence and coercivity on temperature is illustrated in Fig.3. It can be seen from Fig.3a that the remanence reduction of $(\text{Ce}_{0.825}\text{Y}_{0.175})_{13.5}\text{Fe}_{81}\text{B}_{5.5}$ alloy is less than that of pure CeFeB alloy, because the temperature stability of $\text{Y}_2\text{Fe}_{14}\text{B}$ phase is higher than that of $\text{Ce}_2\text{Fe}_{14}\text{B}$ phase. The corresponding temperature coefficient of remanence improves significantly from -0.52%/K to -0.32%/K, increasing by 38.5%. Similarly, the temperature coefficient of coercivity increases considerably from -0.69%/K to -0.41%/K, increasing by 40.6%, indicating that the temperature stability is greatly improved by Y doping.

2.2 Effects of Y and Zr co-doping on magnetic properties and microstructure

Generally, the elements with high melting-point, such as

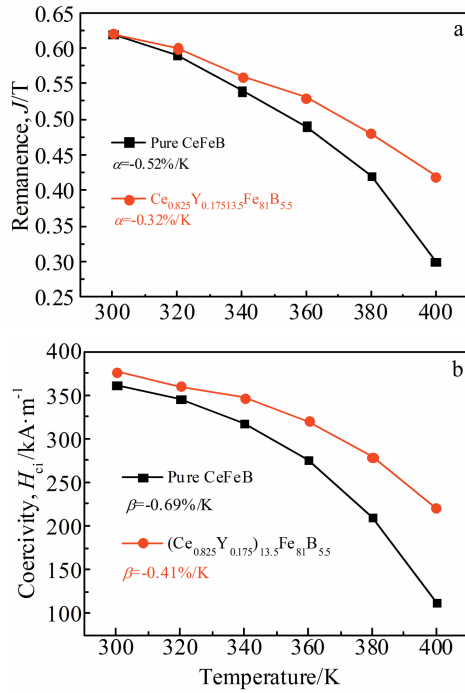


Fig.3 Remanence (a) and coercivity (b) of pure CeFeB and $(\text{Ce}_{0.825}\text{Y}_{0.175})_{13.5}\text{Fe}_{81-y}\text{B}_{5.5}\text{Zr}_y$ alloy at different temperatures

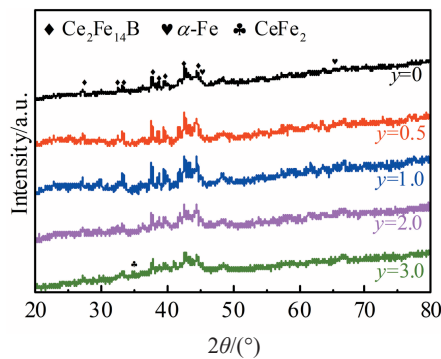


Fig.4 XRD patterns of $(\text{Ce}_{0.825}\text{Y}_{0.175})_{13.5}\text{Fe}_{81-y}\text{B}_{5.5}\text{Zr}_y$ ($y=0\sim 3.0$) ribbons

Nb, Ti, and Zr, can improve the microstructure of alloy [1113], thereby improving the magnetic properties. Based on the above results of Y-doped CeFeB alloys, the effects of Zr addition on magnetic properties and microstructure were investigated. Fig. 4 shows the XRD patterns of $(\text{Ce}_{0.825}\text{Y}_{0.175})_{13.5}\text{Fe}_{81-y}\text{B}_{5.5}\text{Zr}_y$ ($y=0, 0.5, 1.0, 2.0, 3.0$) alloys.

The Zr-doped alloys consist of 2:14:1 phase, α -Fe phase, and CeFe_2 phase. According to Debye-Scherrer formula^[16], the grain size of main phase can be determined as 49.6, 46.2,

44.2, 42.9, and 37.5 nm for $(\text{Ce}_{0.825}\text{Y}_{0.175})_{13.5}\text{Fe}_{81-y}\text{B}_{5.5}\text{Zr}_y$ alloys with $y=0, 0.5, 1.0, 2.0, 3.0$, respectively. Therefore, with increasing the Zr content, the grain size decreases from 49.6 nm to 37.5 nm, and the refined grain size is beneficial for improving coercivity.

Magnetic hysteresis loops and corresponding magnetic properties of $(\text{Ce}_{0.825}\text{Y}_{0.175})_{13.5}\text{Fe}_{81-y}\text{B}_{5.5}\text{Zr}_y$ alloys are demonstrated in Fig. 5. It is noted that the smooth second quadrant demagnetization curves can be observed for all Zr-doped alloys, indicating that these alloys possess strong exchange coupling effect between 2:14:1 phase and α -Fe phase. With the increase of Zr content, the coercivity firstly increases to the maximum value of 407 kA/m, and then decreases to 301 kA/m, as listed in Table 2. The decreased grain size contributes to the increasing coercivity. However, the reduction of coercivity may be attributed to the increase of CeFe_2 phase with further increasing the Zr content. The remanence is decreased with increasing the Zr content, which is attributed to the joint effects from CeFe_2 phase and exchange coupling effect. When $y=2.0$, the maximum magnetic product energy reaches 64 kJ/m³, increasing by 4.9% compared to that of pure CeYFeB alloy. It is concluded that the proper addition of element Zr can improve the magnetic properties considerably. Therefore, after the Y and Zr codoping, the coercivity, remanence, and magnetic product energy improve greatly, increasing by 30.9%, 58.1%, and 204.8%, respectively, compared to those of pure CeFeB alloy.

The fracture SEM images of $(\text{Ce}_{0.825}\text{Y}_{0.175})_{13.5}\text{Fe}_{81-y}\text{B}_{5.5}\text{Zr}_y$ ($y=0\sim 3.0$) alloys are shown in Fig. 6. For all alloys, the size of free surface grains is bigger than that of sticking roller surface grains, which is ascribed to the relatively slow cooling rate in free surface. In general, with increasing the Zr content, the grain size decreases, which is in good agreement with the XRD results.

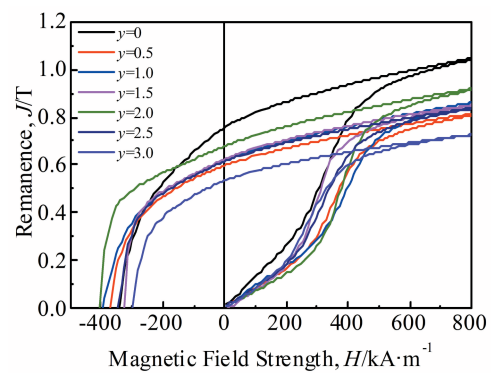


Fig.5 Magnetic hysteresis loops of $(\text{Ce}_{0.825}\text{Y}_{0.175})_{13.5}\text{Fe}_{81-y}\text{B}_{5.5}\text{Zr}_y$ ($y=0\sim 3.0$) alloys

Table 2 Magnetic properties of $(\text{Ce}_{0.825}\text{Y}_{0.175})_{13.5}\text{Fe}_{81-y}\text{B}_{5.5}\text{Zr}_y$ ($y=0\sim 3.0$) alloys

y	0	0.5	1.0	1.5	2.0	2.5	3.0
Coercivity, $H_{ci}/\text{kA}\cdot\text{m}^{-1}$	342	372	395	402	407	346	301
Remanence, J/T	0.76	0.60	0.62	0.58	0.68	0.62	0.53
Magnetic energy product, $BH_{\text{max}}/\text{kJ}\cdot\text{m}^{-3}$	61	48	50	48	64	50	37

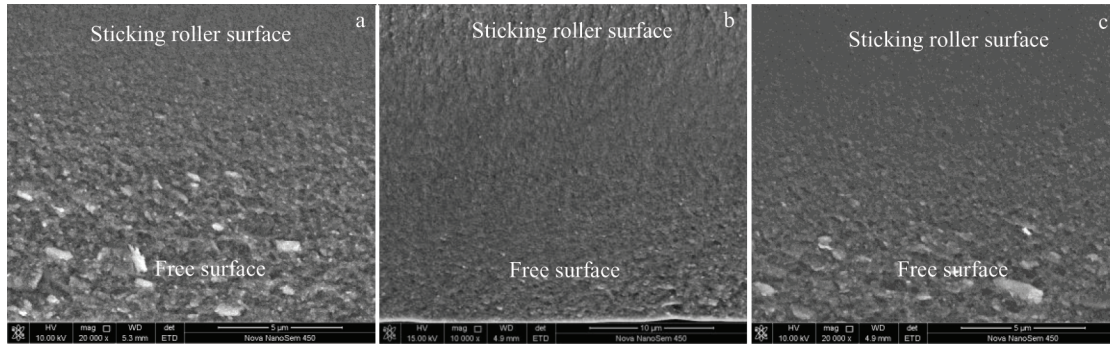


Fig.6 SEM back-scattered images of $(\text{Ce}_{0.825}\text{Y}_{0.175})_{13.5}\text{Fe}_{81-y}\text{B}_{5.5}\text{Zr}_y$ alloys: (a) $y=0$, (b) $y=2.0$, and (c) $y=3.0$

Recoil loops can be determined by removing and applying a successively increasing reversed field on a previously saturated alloy, which can explain the magnetic reversal mechanism. Fig. 7 shows recoil loops of $(\text{Ce}_{0.825}\text{Y}_{0.175})_{13.5}\text{Fe}_{81-y}\text{B}_{5.5}\text{Zr}_y$ ($y=2.0, 3.0$) alloy. In the previous studies, the non-uniform microstructure causes the recoil loops to open, and then magnetic properties decrease^[17,18]. Comparing the $(\text{Ce}_{0.825}\text{Y}_{0.175})_{13.5}\text{Fe}_{81-y}\text{B}_{5.5}\text{Zr}_y$ alloys with $y=2.0$ and 3.0 , the openness of recoil loops for $(\text{Ce}_{0.825}\text{Y}_{0.175})_{13.5}\text{Fe}_{79}\text{B}_{5.5}\text{Zr}_2$ alloy is smaller than that of $(\text{Ce}_{0.825}\text{Y}_{0.175})_{13.5}\text{Fe}_{78}\text{B}_{5.5}\text{Zr}_3$ alloy, suggesting a more uniform microstructure. Thus, the optimal magnetic properties can be obtained for $(\text{Ce}_{0.825}\text{Y}_{0.175})_{13.5}\text{Fe}_{79}\text{B}_{5.5}\text{Zr}_2$ alloy.

According to the relationship $\delta M(H) = M_d(H) - [1 - 2M_r(H)]$, Henkel plots^[19-21] can be used to evaluate the exchange interaction effect. δ is exchange coupling coefficient, M_d represents remanence, and M_r is coercivity. According to

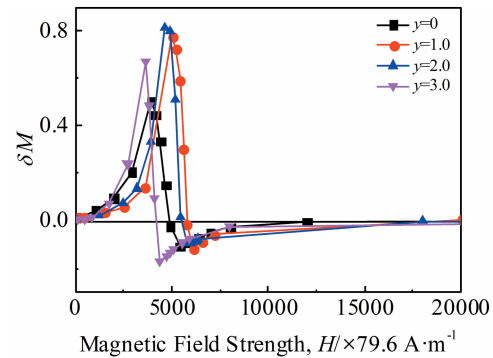


Fig.8 Henkel plots of $(\text{Ce}_{0.825}\text{Y}_{0.175})_{13.5}\text{Fe}_{81-y}\text{B}_{5.5}\text{Zr}_y$ ($y=0\sim 3.0$) alloys

Stoner-Wohlfarth theory^[22], a positive δM value indicates the enhanced exchange coupling, whereas a negative δM value suggests that the magnetostatic interaction dominates when the magnetization reversal occurs. Henkel plots of Zr-doped alloy are demonstrated in Fig. 8. Large positive δM value indicates strong exchange interaction in all Zr-doped alloys, which is confirmed by the smooth second quadrant demagnetization curves, as illustrated in Fig. 5. With increasing the Zr content, the maximum δM value is achieved with $y=2.0$, indicating that the exchange coupling is the strongest.

3 Conclusions

1) The Y addition improves the magnetic properties of CeFeB alloy, and its temperature stability is greatly enhanced. The optimal magnetic properties are achieved for $(\text{Ce}_{0.825}\text{Y}_{0.175})_{13.5}\text{Fe}_{81}\text{B}_{5.5}$ alloy with coercivity of 342 kA/m, remanence of 0.76 T, and magnetic product energy of 61 kJ/m³, which increases by 9.97%, 76.7%, and 190.5%, respectively, compared to those of pure CeFeB alloy. The temperature coefficient of remanence and coercivity is -0.32%/K and -0.41%/K, respectively.

2) The Zr addition refines the grain size of $(\text{Ce}_{0.825}\text{Y}_{0.175})_{13.5}\text{Fe}_{81}\text{B}_{5.5}$ alloy, thereby increasing its coercivity. The excess addition of Zr decreases the magnetic properties due to the formation of CeFe₂ phase. The $(\text{Ce}_{0.825}\text{Y}_{0.175})_{13.5}\text{Fe}_{79}\text{B}_{5.5}\text{Zr}_2$ alloy has good magnetic properties with coercivity of 407 kA/m, remanence of 0.68 T, and magnetic product

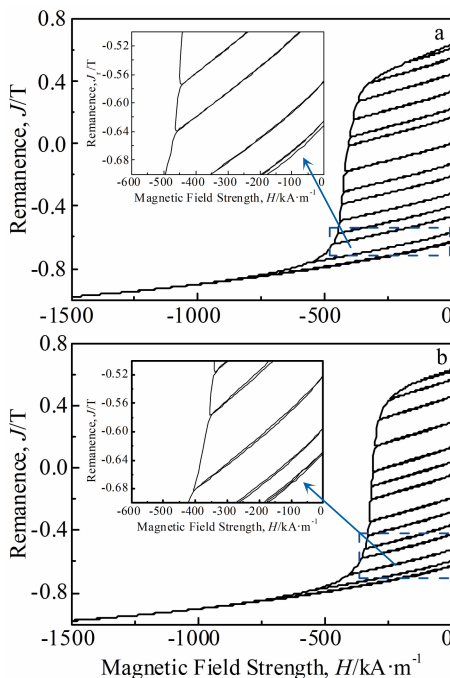


Fig.7 Recoil loops of $(\text{Ce}_{0.825}\text{Y}_{0.175})_{13.5}\text{Fe}_{81-y}\text{B}_{5.5}\text{Zr}_y$ alloys with $y=2.0$ (a) and $y=3.0$ (b)

energy of 64 kJ/m³. The refined grain size and strong exchange coupling effect contribute to the excellent magnetic properties.

References

- Gutfleisch O, Willard M A, Brück E et al. *Advanced Materials* [J], 2011, 42(7): 821
- Hou Y H, Wang Y L, Huang Y L et al. *Acta Materialia*[J], 2016, 115: 385
- Huang Y L, Li Z H, Ge X J et al. *Journal of Alloys and Compounds*[J], 2019, 797: 1133
- Herbst J F. *Reviews of Modern Physics*[J], 1991, 63(4): 819
- Pathak A K, Khan M, Gschneidner K A et al. *Advanced Materials* [J], 2015, 27(16): 2663
- Yang M N, Wang H, Hu Y F et al. *Journal of Alloys and Compounds*[J], 2017, 710: 519
- Jin J Y, Zhang Y J, Bai G H et al. *Scientific Reports*[J], 2016, 6(1): 30 194
- Zhu M G, Li W, Wang J D et al. *IEEE Transactions on Magnetics*[J], 2014, 50(1): 1
- Hirosawa S, Matsuura Y, Yamamoto H et al. *Journal of Applied Physics*[J], 1986, 59(3): 873
- Zhang M, Ren W J, Zhang Z D et al. *Journal of Applied Physics* [J], 2003, 94(4): 2602
- Tang D, Liu Y, Li J et al. *Journal of Magnetism and Magnetic Materials*[J], 2018, 263
- Lin G T, Zhao F, Yu X et al. *Journal of Magnetism and Magnetic Materials*[J], 2020, 504: 166 699
- Wu Q, Pan M X, Ge H L et al. *Journal of Magnetism and Magnetic Materials*[J], 2019, 492: 165 682
- Spyra M, Derewnicka D, Leonowicz M. *Physica Status Solidi A* [J], 2010, 207(5): 1170
- Cui W B, Takahashi Y K, Hono K. *Acta Materialia*[J], 2011, 59(20): 7768
- Zhu J J, Zhou M G, Xu J Z. *Electronic Materials Letters*[J], 2001, 47(1): 25
- Harland C L, Lewis L H, Chen Z. *Journal of Magnetism and Magnetic Materials*[J], 2004, 271(1): 53
- Huang Y L, Shi Z Q, Hou Y H et al. *Journal of Magnetism and Magnetic Materials*[J], 2019, 485: 157
- Chen Q, Ma B M, Lu B et al. *Journal of Applied Physics*[J], 1999, 85(8): 5917
- Liu Z W, Zeng D C, Ramanujan R V et al. *Journal of Applied Physics*[J], 2009, 105(7): 926
- O'Grady K, El-Hilo M, Chantrell R W. *IEEE Transactions on Magnetics*[J], 1993, 29: 2608
- Wohlfarth E P. *Journal of Applied Physics*[J], 1958, 29(3): 595

Y和Zr掺杂对CeFeB合金微观结构和磁性能的影响

周艳霞, 李 伟, 符小坤, 侯育花, 黄有林
(南昌航空大学 材料科学与工程学院, 江西 南昌 330063)

摘 要: 研究了Y和Zr掺杂对CeFeB合金相组成、磁性能和温度稳定性的影响。结果表明, CeYFeB合金由2:14:1主相和少量 α -Fe相组成。Y掺杂可有效提高合金的矫顽力、剩磁和最大磁能积。同时由于Y₂Fe₁₄B相优异的磁性能与高温稳定性, 其温度稳定性也得到明显改善, 掺杂后合金的剩磁和矫顽力温度系数分别为-0.32%/K和-0.41%/K, 与纯CeFeB合金相比分别提高了38.5%和40.6%。Y和Zr共掺杂后, 由于增加的磁晶各向异性场和晶粒尺寸细化所产生的联合效应, 合金的矫顽力、剩磁和最大磁能积大幅度提高, 分别比纯CeFeB合金提高了30.9%、58.1%和204.8%。

关键词: CeFeB合金; Y掺杂; Zr掺杂; 磁性能

作者简介: 周艳霞, 女, 1994年, 硕士生, 南昌航空大学材料科学与工程学院, 江西 南昌 330063, E-mail: 2521631500@qq.com